academicJournals

Vol. 9(10), pp. 233-242, 30 May, 2014
DOI: 10.5897/IJPS2013.4084
Article Number:776F63545011
ISSN 1992 - 1950

http://www.academicjournals.org/IJPS

International Journal of Physical Sciences

Full Length Research Paper

Study of vibrations by Raman spectroscopy low frequencies of the phase transition in pyridinium picrate $(C_6H_2N_3O_7)^-.(C_5H_6N)^+$

AZIZI Abdelkader* and MEDDOUR Athmane

Department of Physics, Faculty of M. I. S. M, 08 May 1945 University, BP 401, Guelma 24000, Algeria.

Received 02 December, 2013 ; Accepted 14 February, 2014

The spectra of the crystals of pyridine picrate crude formula, $C_{11}H_8N_4O_7$, in the mid infrared (IR) and Raman are studied as a function of temperature. They show some changes, which allowed us to first track and describe the structural changes (in both directions under the effect of heat treatment) accompanying the phase transition between 358 and 383K observed by DSC, Rx. After gradual cooling, the reversibility of the alteration may be detected by the variation 1'etude frequencies and relative heights of the lines connected to groups of bands NO_2, NH and CH. The results show that the transformation kinetics is influenced by the operational conditions.

Key words: Picrate pyridine transition phase, reversibility, infrared (IR), Raman, X-ray diffraction (XRD).

INTRODUCTION

Pyridinium picrate has properties which make it useful in various fields such as biology, optics, catalysis; it is also used for purification in the pharmaceutical industry. Hence, it is necessary to know the importance of the thermal stability of the two phases or the polymorphic behavior of the active substance in order to optimize operation and storage conditions so that only the desired shape is seen in the processes.

This work contributes to the study of phenomena related to the dimorphic of an organic salt called 'picrate pyridine' $[(C_6H_2N_3O_7)^-.(C_5H_6N)^+]$ by comparing the behavior of its two forms, named Phases I and II, respectively. This is done to provide additional structural and spectral data to previous results of other authors, by monitoring the behavior and activity of any group of spectroscopy essential for the understanding of its mechanism of structural changes in order to address the question of reversibility of this transition. To do this, a particular technique was preferred: Raman spectroscopy. It has the ability to provide guests with information on the molecule structure, its binding mode and the presence or absence of an interaction; this makes particular interesting target to be influenced by particular groupings of transition phase phenomena. This works aims to complement the studies of the structural data of this dimorphic. This is because till date, there is no comprehensive study on the vibration spectra of crystals, PicPy. The unusual work is essentially based on X-ray diffraction (XRD), which we made reference to in this study (Botoshansky et al., 1994; Talukdar and Chaudhuri, 1976).

*Corresponding author. E-mail: azizikader@yahoo.fr

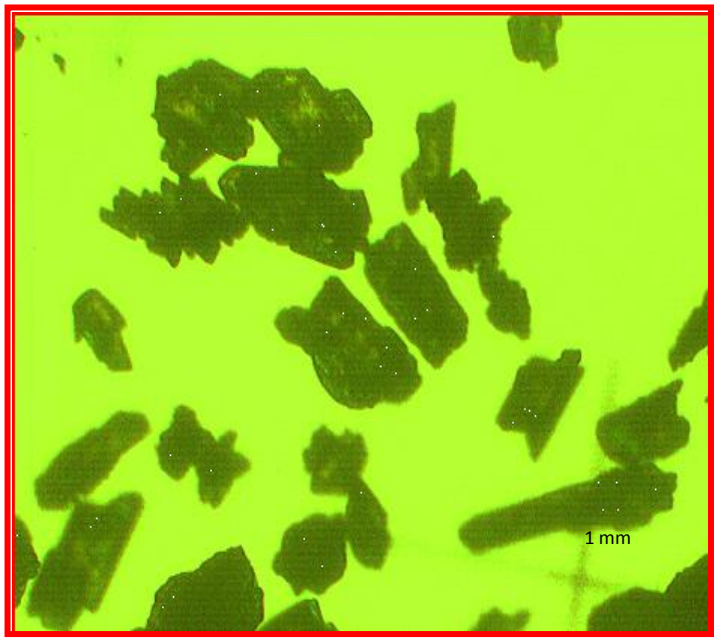

Figure 1. Micrograph of crystals ambient (yellow).

EXPERIMENTAL DETAILS

Synthesis and preparation of crystals

The synthesis powder was made by precipitation. This involves slow evaporation of saturated solution of a stoichiometric mixed with reagents (202 g of picric acid and 0.8 g of pyridine). Yellow crystals that stain were grown after being filtered in a vacuum and then were weighed. 204 g of crystals with a yield of 97% (precipitation rate) was obtained. This product is stable and can be handled in open air without any special precautions. The micrograph of the crystal analysis (Figure 1) shows that the product obtained does not have very regular form, but the major fraction of the population of these crystals has an average size of 0.9 × 0.8 × 0.04 mm^3.

It is already remarked that during the preparation, the crystals change color when exposed to relatively high temperatures of around 363K (boiling solvent) for about 10 min. The coloration of the crystals changes from light yellow to brown. The same color change was observed by Mark et al. (1994).

Thermal analysis by differential scanning calorimetry

For structural characterization, it is very important to start with the study of thermal behavior in order to identify areas of stability and transition, highlight thermal anomalies revealing any change in these properties under the influence of the thermal environment. For this purpose, we used first thermal analysis by differential scanning calorimeter.

The curves were obtained on a sail Labsys Evo TG- DSC, with a mass of 35 mg of sample in an aluminum crucible and in a measuring cell with a capsule called a reference. They were subjected to a temperature program ranging from 293 to 424K, as ramps 285, 283 and 281K/min under nitrogen atmosphere (35 ml/min). These curves (Figure 2) show that at the beginning of 358K, thermal activity gives rise to a first endothermic peak center of 368K, which is the melting starting point of Phase I, followed by an exothermic peak intermediate between the two bands (endothermic), which combine a recrystallisation solution Phase II with a second endothermic peak at 383K. The melting peak does not appear on the curve, being a limited temperature of 423K. This is done to prevent degradation of the product in the device and thus damaging its smooth operation.

In both endothermic points, the hypothesis of the formation of Phase II, following the merger of Phase I at the same temperature (358K) is given by Mark et al. (1994) and Talukdar and Chaudhuri (1976); this gave us an idea of the areas in which the temperatures must focus on for XRD, infrared (IR) and Raman records. It is noted that the recordings done by cooling the samples at these speeds show no sign of activity.

Diffraction X -ray powder (XRD)

To control the structure, it is ensured that the compounds prepared in the expected system are well crystallized. Two samples were prepared; one was stored at room temperature (293K) and the other treated in an oven at a temperature of 368K for 30 min (in order to cause the transition phase). They were characterized by XRD using a diffract meter operating with copper Kα radiation (λ = 1.5406 Å). The records obtained are shown in Figure 3.

The indexing of the experimental peaks of diffractograms was done by using the program Mercury CCDC and ASTM (02-068-1154). The refinement of the cell parameters of Phase I (at room temperature) shows that it crystallizes in a monoclinic system, space group $P2_{(1)/c}$, with lattice parameters,

a = 12.122(2) Å; b = 3.7830(10) Å; c = 26.621(3) Å;
α = 90°; β = 92.56°(5); γ = 90° et Z = 4, Z' = 4.

and at the processing temperature of 368K for 30 min (the transition Stage II) in a triclinic system, space group P-1 with cell parameters:

a = 10.156(2) Å; b = 8.984(2) Å; c = 7.2300(10) Å ;
α = 86.38(5)°; β = 80.10(5)°; γ = 89.97(5)° et Z = 2, Z' = 0.

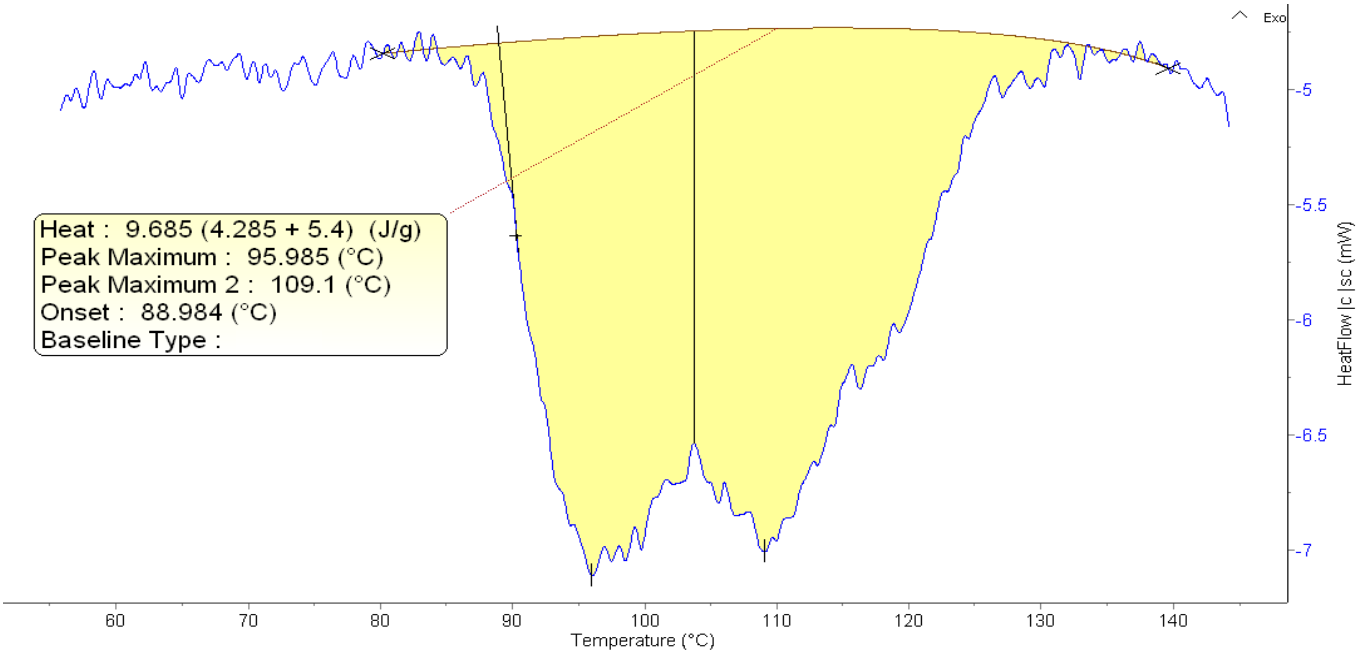

Figure 2. DSC thermograms.

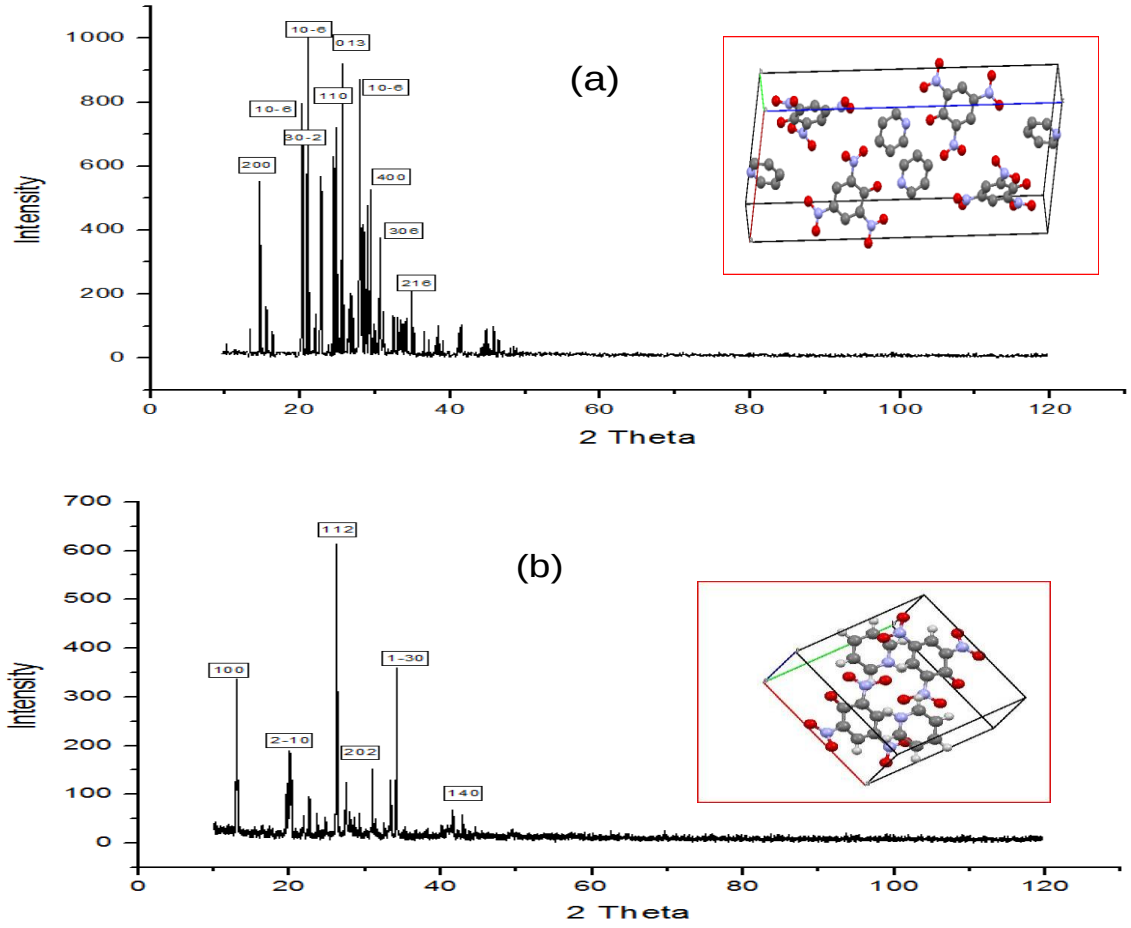

Figure 3. XRD diffractograms of the samples treated for 30 min at temperature **(a),** 298K; **(b),** 368K.

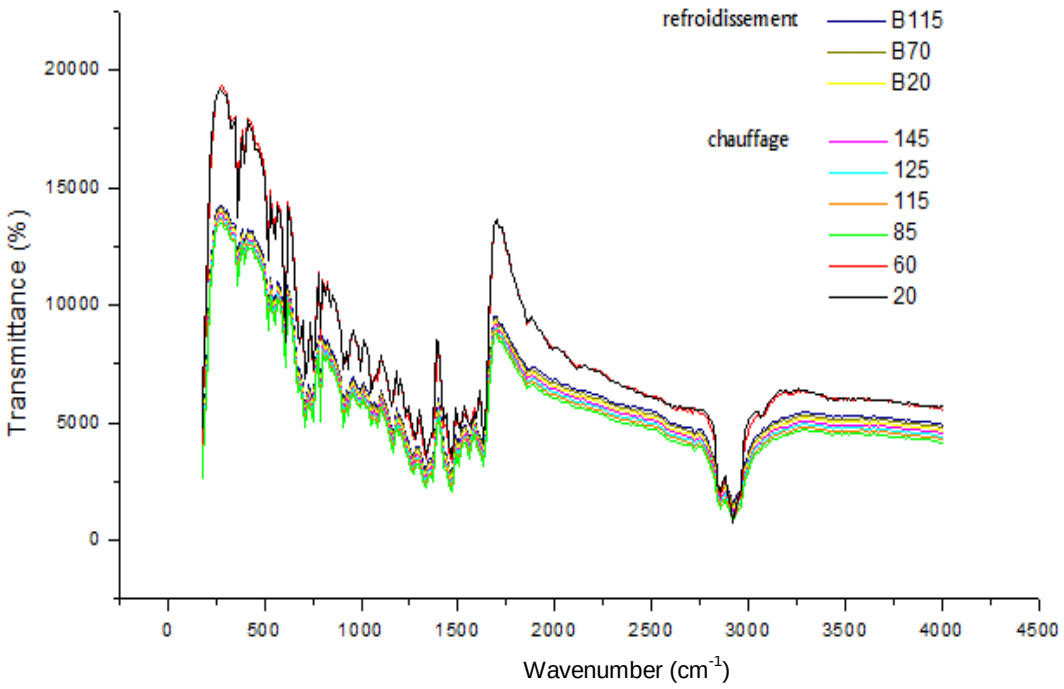

Figure 4. Influence of temperature on the IR transmission spectra 293, 333, 358.398 and 418K (During heating); B115 and B388, B343 and B29 (during cooling).

RESULTS AND DISCUSSION

Vibrational spectroscopic study

IR and Raman spectroscopy recorded as a function of temperature (and time), the frequency domain initially scanned and the samples are in the form of powder in suspension in Nujol. To monitor the behavior and check the reversibility of the process of phase transition upon cooling, IR spectra were recorded on heating at temperatures going from ambient to 418K (293, 333, 358.398 and 418K); but during gradual cooling, the temperatures were lowered (B388, B343 and B293). The aim is to record spectra at critical temperatures, where we observed the thermal anomalies on the DSC curves. Figure 4 shows the transmittance spectra.

In general, we observe two sets of parallel spectra with the same speed and bands. The spectra recorded at 293 and 333K are very similar and they fit perfectly. So we think that there is no change. However, at 358K, the spectra are slightly modified compared to those recorded at lower temperatures; and beyond 358K, the recordings are also almost identical with that recorded at 388, 398 and 418K. However, there are differences between the massive 600 and 800 cm^{-1}, around 1450 cm^{-1} and 1350 cm^{-1} and between 1400 and 1750 cm^{-1}.

At 388K, there is a remarkable evolution of the spectra; there is contrast reversal of intensities between 600 and 400 cm^{-1}; we note that the number of bands decreased for regions between 850 to 750 cm^{-1} and 1350 to 1750 cm^{-1}.

Attempting IR bands award

The complexity of the crystal structures of the complete assignment makes each PicPy very delicate peak. In comparison with previous work and studies conducted on similar complexes and databases in the literature, it was possible to assign most of the peaks. Table 1 summarizes the main groupings.

IR spectra composed were compared with the Raman spectra (Figure 5) based on the thermal variations or anomalous thermal survey on the DSC curves and on the basis of two XRD diffractgrams. The spectra are shown in Figure 6 for two temperatures: ambient (raw sample) and 368K. The vibration spectra show much mark than the IR spectroscopy with 368K temperature differences. We note that bands are fewer and have more specific characteristics and locations.

It is evident that the spectra consist of two frequency ranges, with changes of matter; spectral region between 110 to 1500 cm^{-1} mode field elongation CC bonds and strain CN 1140 to 1180 cm^{-1} field user elongation CC bonds. Fine deformation peak is recognized in the planes of the groups NO_2 and 820 cm^{-1}, which is observed with no decrease in the intensity change of position (Varsanyi, 1974).

The strips 711 (IR) and 721 cm^{-1} (R) have very low intensity of vibration in the plane deformation of C-H bonds; the rocking vibration in the nuclei is observed at 912 cm^{-1}. The CC stretching vibrations of the cycle are relatively small and are located at 1592, 1506, 1460 (IR),

Table 1. Summary of the main award bands (Varsanyi, 1974; Silverstein et al., 1991; George Socrates, 2004; Roeges, 1994)

Frequency (cm^{-1})		Attribution
Phase I	**Phase II**	
3095	3080	v C-H ring str
1631	1630	v C-C ring str
1571 1555	1563 1553	v asym NO_2
1486 1477	1506 1461	v C-C ring
1365 1346	1367 1345	v sym NO_2
1283	1266	v phen C-O
- 822	837 819	δ NO_2
742	745	NO_2 wag.
695	678	γ_w C-C
516	514	γ NO_2

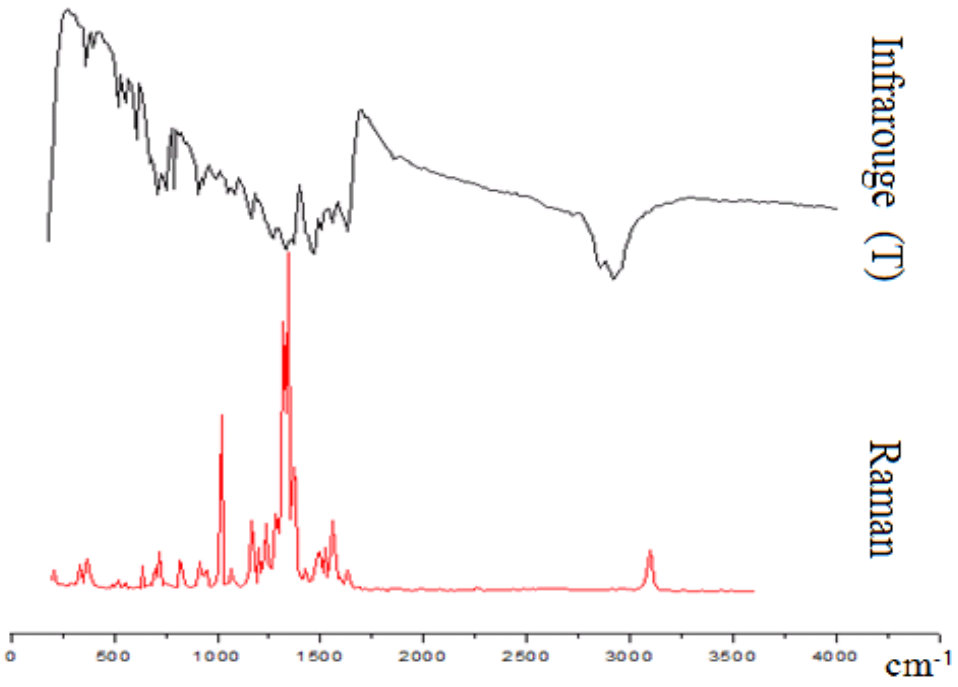

Figure 5. Comparison of IR and Raman spectra PicPy 293K.

1477 (R) cm^{-1} and bending modes between 690 and 730 cm^{-1}. Other modes of deformation are observed by a small band of 1266, 1073, 1018, 1000 and 786 cm^{-1} (Silverstein et al., 1991; George Socrates, 2001).

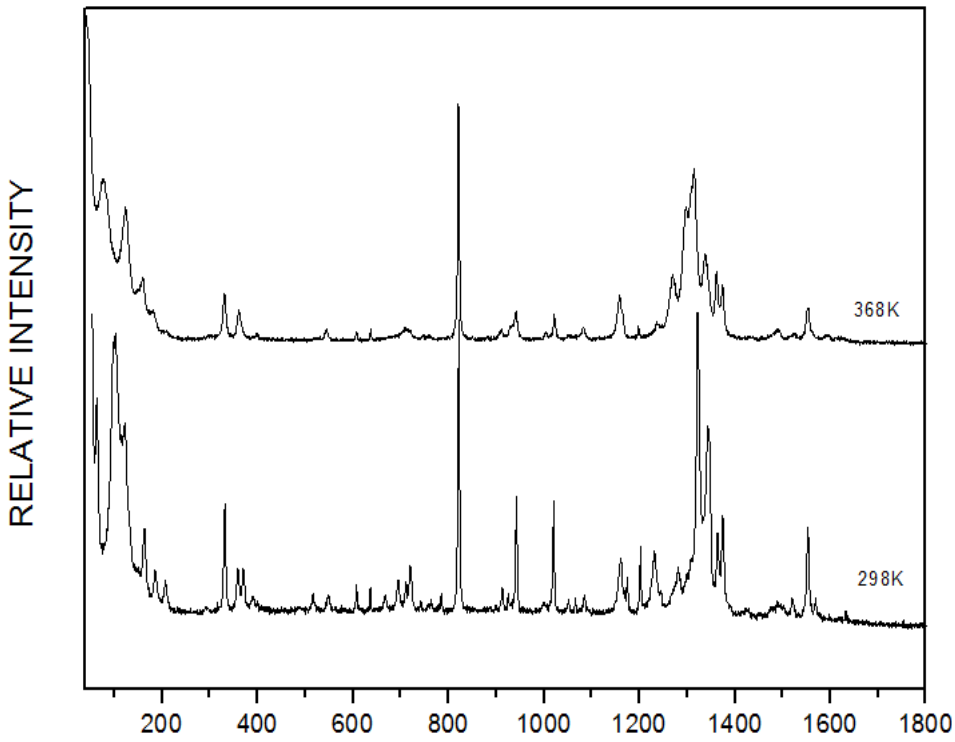

Figure 6. Raman spectra for two temperatures 298 and 368K.

Duplication of core bands around 360 cm^{-1} is assigned to the stretching vibration mode of the CNC pyridine. The position of these bands is fixed and the intensity is greatly changed. Because the intense and broad absorption is centered around 1325 cm^{-1} with several shoulders, this mass slides, by effect of temperature and its width, decreases considerably with several shifts of these peaks. These shifts cause changes in the spectroscopic band profile and intensity, gang evolution with temperature and a shift towards lower frequencies of the Raman band at 796 cm^{-1}; elongation binding depending on the temperature, and the opening angle between the cation-anion to the low wave numbers where collective movements occur (Gunter and Tuan, 2008; Kalsi, 2004).

ANALYSIS BY RAMAN SPECTROSCOPY (LOW FREQUENCY MODES)

In Raman spectrometry, in particular, lower region of less than 250 cm^{-1} frequency, and said network users (external or modes) that are due to the movements of translation and rotation of the molecules in the crystal lattice are bands stretching vibrations (CH and L.H. groups) that are very sensitive to intra-and intermolecular arrangement, as amended within and outside plane of the ring and vibration of aromatic rings themselves. For this purpose, recordings are made on Raman spectroscopy of the samples in sealed tubes, using an excitation wavelength of 1.06 microns (IR), obtained with a laser having an output of 60 mW in the laser output, a spectral between 05 and 4000 $cm^{-1.}$

Raman spectra as a function of temperature

A. During heating

Raman registered for different temperatures (Figure 6) spectra clearly shows the existence of two distinct crystalline forms (Phases I and II), previously identified by XRD patterns (Figure 3); in some disturbance vibration modes reflection, one notices a structural change or transition. Figure 7 shows the shape of the spectra and their changes as a function of increasing temperature in a range going from 298 to 443K records on heating and cooling (Varsanyi, 1974; Silverstein et al., 1991).

The Raman spectra (Figure 7a) are mainly composed of two stage types. In the first, there is a series of fine and intense peaks below 75 cm^{-1}, located at 22, 30, 50 and 63 cm^{-1}. They are mostly due to movements involving more groups in the form of couplings (torsion deformation). The few internal vibrations of relatively high frequency are also detected in the form of relatively broad bands, a second region composed of higher frequencies by two broad bands at 100 and 123 $cm^{-1,}$ in shoulder form with small secondary strips at 164, 186, and 205 cm^{-1}.

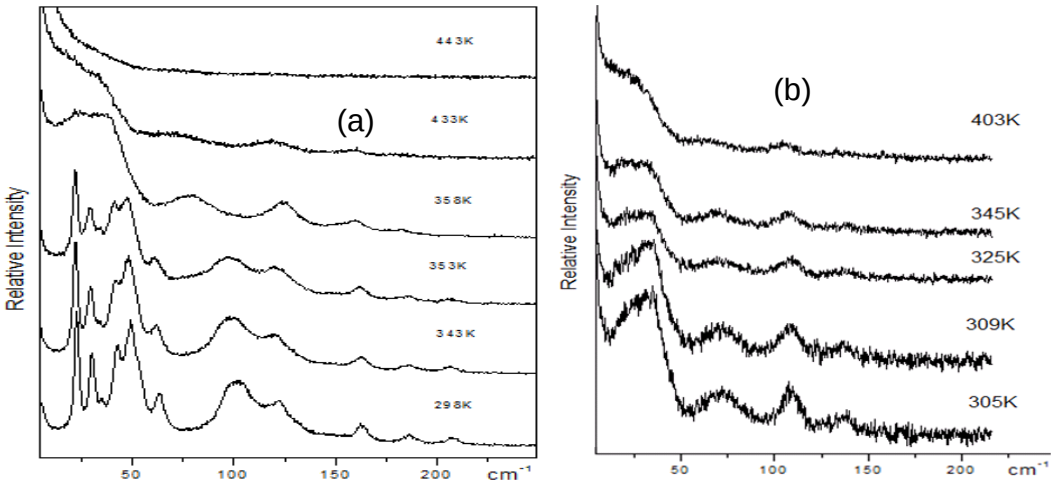

Figure 7. Raman spectra at different temperatures (low frequencies) (a) heating (b) cooling.

Table 2. Assignment of low frequency modes.

Frequency (cm^{-1})	Attribution
22.5	-
30	-
35.2	-
40-50-60	τ NO_2
100	L.H , *δs*(CH)
120	γ (C-C-C)
165	β(C-NO2)
186	β(C-O),
205	β(C-NO_2)

ν: Elongation; **β, γ:** deformation dans et hors plan; **γ_w:** balancement hors plan.

These secondary peaks disappear during increase in temperature (beyond 353K). We note the changing profile of the main lines of the first region, which is seen to expand and form a broad bump with total recovery. Remember that bump is called the amorphous specific Boson. Also, two interesting bands at 60 and 100 cm^{-1} give rise to a weak band center of 75 cm^{-1}; extremely weak bands (Figure 7b) and small bands of 164, 186 and 205 cm^{-1} tend to disappear (or vice- versa tape). The observed frequencies and their allocation are reported in Table 2. This development is interpreted by steric effects and structural deformation and then by the transition from monoclinic to triclinic structure.

B. During cooling

Spectra have also been recorded during cooling, at the following temperatures: 403, 345, 325, 309 and 305K. The obtained recordings are represented in Figure 4b. They always appear in Structure II with side bands of 300, 200 and 120 cm^{-1} and whose intensity is inversely with changes in temperature. Furthermore, we note the emergence of a wide strip resulting recovery bands is 37 cm^{-1}. This means that the phenomenon of transition dimorphic is not irreversible to Phases II and I (in these operating conditions). At the end, at 433 and 443K temperatures, melting resulted in the complete absence of peaks.

The crystal structure through the main lines keeps up the temperature of 353K (80°C) and then forms a large mass center at 40 cm^{-1}, which has a smooth assignment of the structural arrangement. In fact, when the temperature increases, there is distortion of the crystalline structure by displacement of the frequencies of vibrations in the direction of decreasing the angle between cation-anion through hydrogen bonding. This is less rigid, thus reducing the vibration frequency of hydrogen bond. As shown in Figure 7a, b, it is from 100 cm^{-1} for 293K and 75 cm^{-1} for 403K

Profiles of some parameters

Figure 8 illustrates the information in the changing frequencies of the lines of the Raman spectra as a function of temperature. In the first movement, it is found that V1 to V4 modes have no frequency that is substantially stable (frequency is insensitive due to temperature). On the other hand, the higher frequency mode has a slight growth with a problem of bending to around 345K; band is denoted as V6; they pass about 64 cm^{-1} at 289K to 100 cm^{-1} at 353K. This shift results from all disturbances which bring structural changes.

Then, the intensity of these lines varies inversely with temperature, but with a large difference between the slopes (the attenuation bands). V5 and V7 modes show a

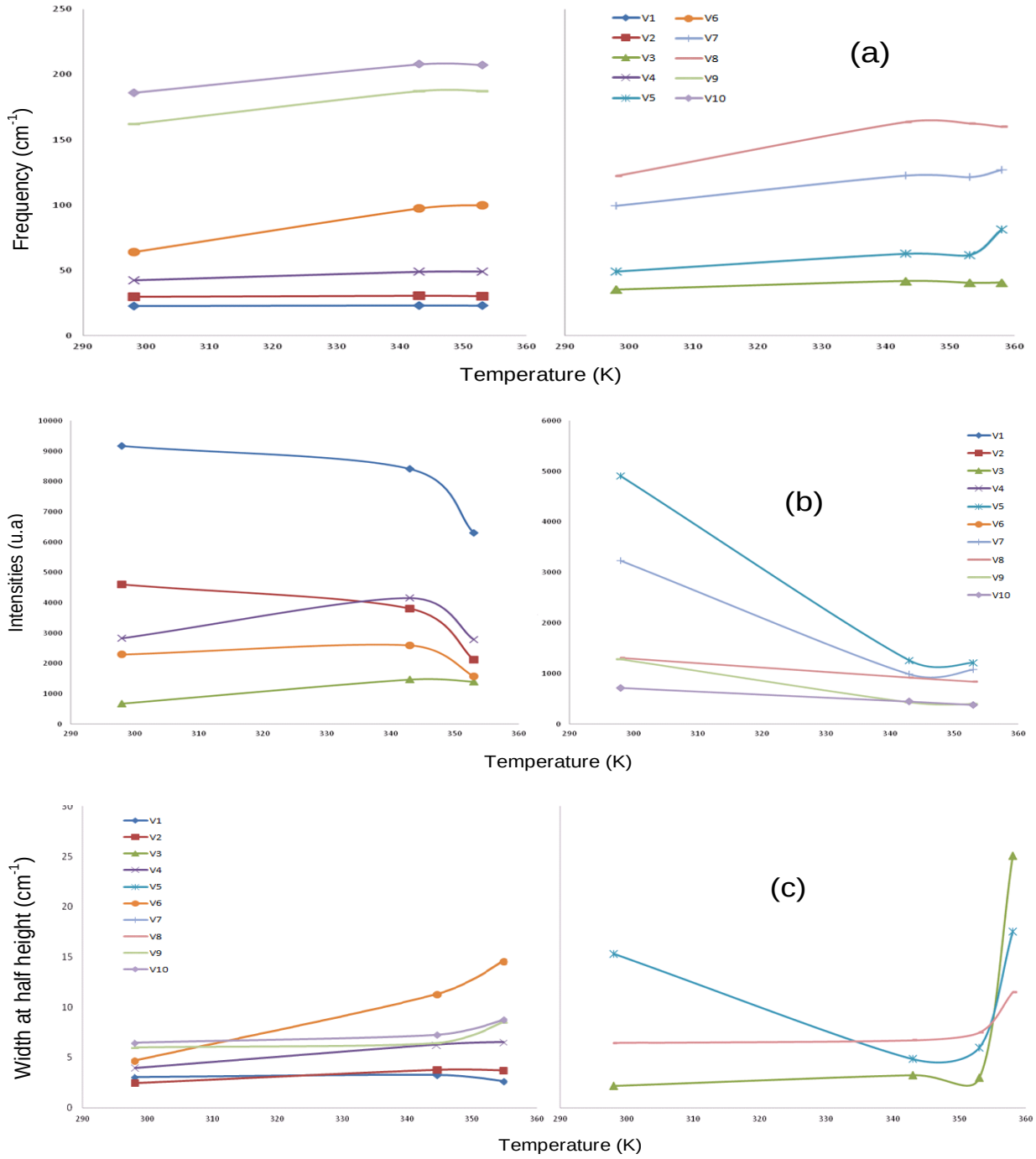

Figure 8. Variation in function of the temperature (a) Frequency (b) intensities and (c) the width at half height of the different modes (<250 cm^{-1}).

great decrease in the frequencies between 300 and 340K; this reduction becomes relatively less pronounced in modes V1 and V4, when the temperature is above 340K; other modes decrease almost linearly with a slope change in the vicinity of the same temperature. Figure 8c illustrates the monitoring of the behavior of the width at half height of the peaks depending on the temperature. It is noted that this parameter varies little in absolute value in terms of peak low frequency V1, V2 and V4 with a variation of about 5 cm^{-1}. This is unlike that of the V5 and V3 modes, wherein the width at half height of the peaks shows a rapid increase with enlargement of the passage and temperature of 350K. An inflection point is observed with a more rapid increase. These parameters are full

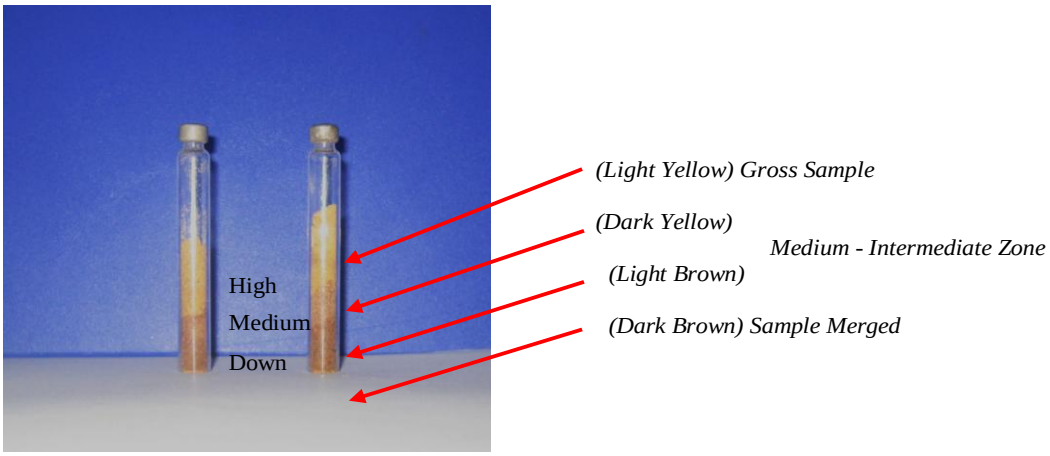

Figure 9. Sealed tubes brought to fusion at their end in a furnace.

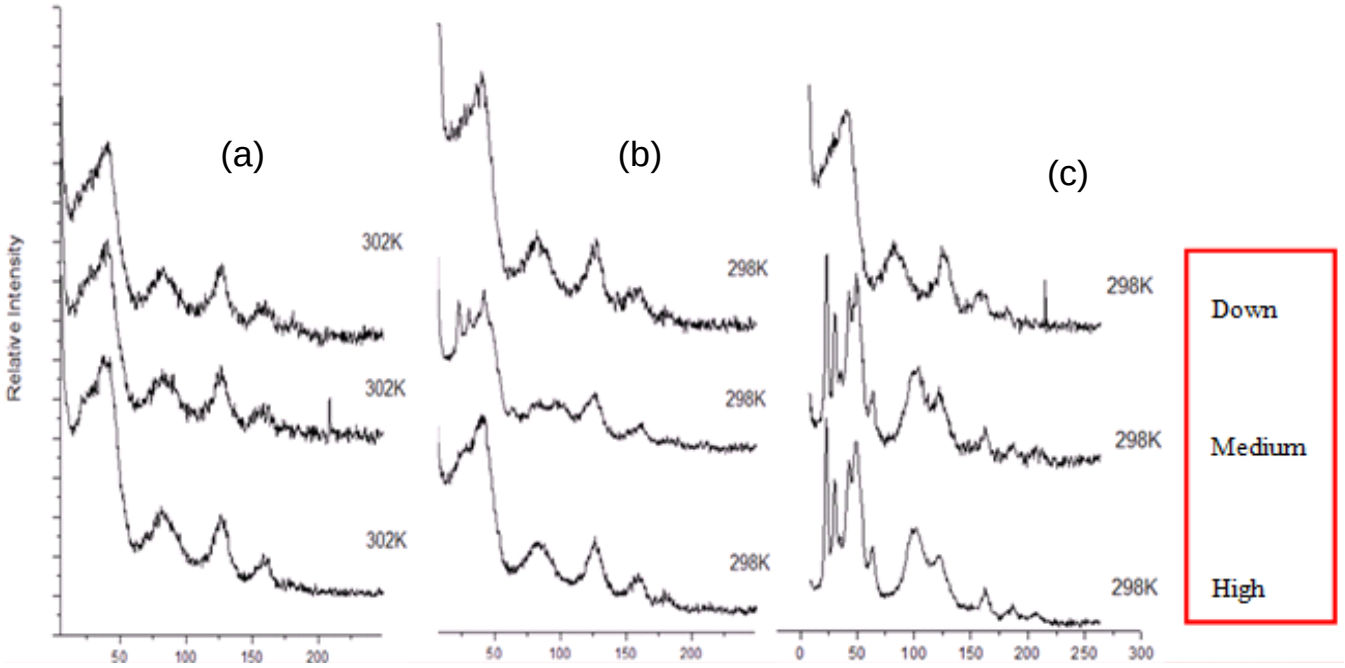

Figure 10. Evolution of the Raman spectra as a function of time (constant temperature), after 30 min (b) after 24 h (c) after 48 h.

information, particularly sensitive to the nature of the arrangements and connections. These abnormalities affecting the variation width at half height and the variation mode V5 frequencies are indicative of the existence of a phase transition at a temperature of about 345K.

Study of the evolution of the Raman spectra of time

Figure 9 shows the samples having different zones formed after treatment of the lower end of tube (sealed) in an oven at 443K for 30 min.

In general, the structure is retained when the room temperature (between 293 and 303K) is kept for a while and going up after 24 h (Figure 10a and b); by cons, it changes structure involved in the case where the sample is held in the sealed tube for a period of 48 h (Figure 10c). It is now apparent that the spectra have the same lines, speeds and equal intensity that start the sample 47 (a) at lower temperature (353K) almost together. Under these conditions, there is crystallization of Phases I in Phase II.

The Raman spectroscopy in Figure 11 demonstrates the reversibility of the phenomenon of transition. That is to say, in the recovery of the structure of the Phase I, the

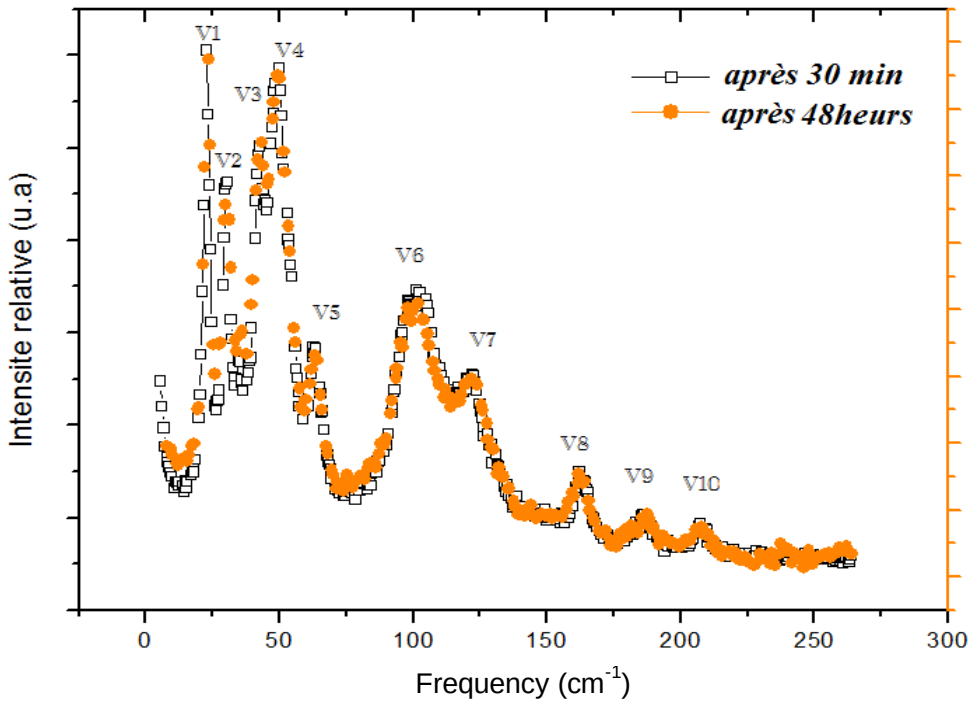

Figure 11. Comparison of the spectra of a sample before treatment and after treatment 433K.

two spectra, in fact, the crude sample was kept ambient and the other at 30 min and 48 h. They were maintained in the cell after the ambient undergoes treatment at 433K (170°C); they are identical and fit perfectly in position and intensity.

Conclusion

This study provides useful information on the nature of the transition and structural relaxation mechanism; in particular, those related to NO_2 groups, NH and CH, involved during the transition. We have discussed the relationship between the internal and phase transition mode, the dependence of frequency width at mid-height and the intensity of the band, depending on the temperature, with a common point in the immediate vicinity of 360K. There are signs of 1'existence of structural change. This affects both mode networks (external mode) and the internal vibration modes. However, in the second part of this study, after gradual cooling of the sample and holding for several hours (48 h) at room temperature, the time required for relaxation is the presence of reversibility, as evidenced by the reappearance of the strips. After relaxation under these operating conditions, the spectra of form I do not evolve with time.

Conflict of Interests

The authors have not declared any conflict of interests.

REFERENCES

Botoshansky M, Herbstein FH, Kapon M (1994). Pyridinium picrate - the structures of phases I and II. Correction of previous report for phase I. Acta Crystallographica, Section B. 50:191-200. http://dx.doi.org/10.1107/S0108768193008584

George Socrates (2001). Infrared and Raman characteristic group frequencies table and chartes. Wiley: Middlesex, UK.

Gunter G, Tuan VD (2008). Handbook of Spectroscopy. Volume 1. pp. 39-45; 100-110.

Kalsi PS (2004). Spectroscopy of Organic Compounds new age international publishers 6TH edition.pp. 87-162.

Mark B, Frank HH, Moshe K (1994). Crystallography of metal picrates. II. Crystal structure of yellow thallium(I) picrate; relations among various M(I) picrate phases. Acta Cryst. B50:589-596. http://dx.doi.org/10.1107/S0108768194001746

Roeges NPG (1994). A guide to the complete interpretation of infrared spectra of organic structures, Wiley: New York.

Silverstein RM, Bassler GC, MORRILL TC (1991). Spectrometric Identification of Organic Compounds 5th Ed. John Wiley. New York. 1991.

Talukdar AN, Chaudhuri B (1976). The crystal and molecular structure of pyridine picrate. Acta Cryst. B32:803. http://dx.doi.org/10.1107/S056774087600397X

Varsanyi G (1974). Assignments of vibrational spectra of seven hundred benzene derivatives, Wiley: New York.